Wind Energ. Sci. Discuss., doi:10.5194/wes-2016-55, 2017
Manuscript under review for journal Wind Energ. Sci.
Published: 2 January 2017

eawe european academy of wind energy
Open Access WIND ENERGY SCIENCE DISCUSSIONS

Joukowsky actuator disc momentum theory

Gijs van Kuik
Duwind, Delft University of Technology, Kluyverweg 1, 2629HS Delft, NL
Correspondence to: Gijs van Kuik (g.a.m.vankuik@tudelft.nl)

Abstract. Actuator disc theory is the basis for most rotor design methods, be it with many extensions and engineering rules added to make it a well-established method. However, the off-design condition of a very low rotational speed Ω of the disc is still a topic for scientific discussions. Several authors have presented solutions of the associated momentum theory for actuator discs with a constant circulation, the so-called Joukowsky discs, showing the efficiency $C_p \to \infty$ for the tip speed ratio $\lambda \to 0$. The momentum balance is very sensitive to the choice of the vortex core radius δ as the pressure and velocity gradients become infinite for $\delta \to 0$. Viscous vortex cores do not show this singular behaviour so an inviscid core model is sought which removes the momentum balance sensitivity to singular flow. A vortex core with a constant δ does so. Applying this in the momentum balance results in $C_p \to 0$ for $\lambda \to 0$, instead of $C_p \to \infty$. At the disc the velocity in the meridian plane is shown to be constant. The Joukowsky actuator disc theory is confirmed by a very good match with the numerically obtained results. It gives higher C_p values than corresponding solutions for discs with a Goldstein-based wake circulation published in literature.

1 Introduction

Although the concept of the actuator disc is more than 100 years old, it is still the basis for rotor design codes using the blade element momentum theory developed over these 100 years, see van Kuik et al. (2015). In recent years the behaviour of actuator disc flows with a low rotational speed has been studied by several authors, providing several solutions depending on the type of load that is applied, see e.g. Sørensen (2015). Research has focussed on rotors and discs having a constant circulation in the wake, known as the Joukowsky distribution (1918), or the Betz distribution (1927) yielding a helicoidal wake structure moving with a uniform axial velocity. Goldstein (1929) was the first to find a solution for this wake for lightly loaded propellers, see Okulov et al. (2015) for an overview. Both distributions were assumed to represent the circulation distribution of an ideal rotor. The present paper considers the Joukowsky distribution and compares the results with solutions of the Betz-Goldstein distribution modified for heavily loaded actuator discs reported in Okulov and Sørensen (2008); Okulov (2014) and Wood (2015).

The swirl of the wake is induced by a discrete vortex at the wake centre line, leading to an infinite azimuthal velocity and pressure for the radius $r \to 0$. The question how to model the discrete vortex and how this impacts the momentum balance has been studied by e.g. de Vries (1979); Sharpe (2004); Xiros and Xiros (2007); Wood (2007); Sørensen and van Kuik (2011). All performance predictions reported in these references show a remarkable result: in the limit to zero rotational speed the efficiency of the disc increases to infinity, which is highly non-physical.

Wind Energ. Sci. Discuss., doi:10.5194/wes-2016-55, 2017
Manuscript under review for journal Wind Energ. Sci.
Published: 2 January 2017

eawe european academy of wind energy
Open Access WIND ENERGY SCIENCE DISCUSSIONS

Within the inviscid flow regime, the analysis in Sørensen and van Kuik (2011) is considered to be exact apart from the choice of the vortex core at the axis of the wake. The centreline vortex is a Rankine vortex of which the core diameter is proportional to the wake radius. Their analysis shows that adding a disturbance parameter to the momentum balance removes the non-physical result of infinite efficiency for zero rotational speed, no matter how small this disturbance is. This is an indication that the momentum balance is very sensitive to small deviations in the flow parameters.

A failed attempt to reproduce the results of Sørensen and van Kuik (2011) by the potential flow actuator disc code described in van Kuik and Lignarolo (2016) initiated a re-analysis of the vortex core model and its impact on the momentum theory. In section 2 the equations of motion for Joukowsky actuator disc flows are given as well as for the disc loading and far wake properties. Herewith the general mass, momentum and energy balances are derived in section 3.1, followed by section 3.2 where the vortex core model is analysed. The chosen core model is applied in section 3.3. Section 4 describes the numerical approach of which the results are presented in section 5 and compared with the momentum theory results in section 6.

2 The equations of motion

2.1 The equations for a disc with constant circulation

The flow is governed by the Euler equation:

$$\frac{1}{\rho}(\boldsymbol{f} - \boldsymbol{\nabla} p) = \boldsymbol{v} \cdot \boldsymbol{\nabla} \boldsymbol{v} \tag{1}$$

in which ρ is the fluid density [kg/m^3], f the force density [N/m^3], p the static pressure [N/m^2], $\boldsymbol{v}$ the velocity vector [m/s] and $H = p + \frac{1}{2}\rho \boldsymbol{v} \cdot \boldsymbol{v}$ the total pressure [N/m^2]. Also the equivalent formulation:

$$\boldsymbol{f} = \boldsymbol{\nabla} H - \rho \boldsymbol{v} \times \boldsymbol{\omega} \tag{2}$$

will be used. A cylindrical reference system (x, r, φ) is applied, with the positive x coinciding with the downwind wake axis, and with r and φ the radial and azimuthal coordinate, see figure 1. For the special case of a disc flow with constant circulation induced by a free vortex Γ at the axis of the wake the azimuthal velocity in the wake is:

$$\Gamma = 2\pi r v_\varphi. \tag{3}$$

The vortex is a potential flow vortex, with a vortex core having diameter $\delta(x)$. It is common to model the core as a Rankine vortex, characterized by solid body rotation of the flow, after which the limit of $\delta \to 0$ is taken. Figure 1 shows (half of) the cross section through the stream-tube in the meridian plane, with the disc and fully developed wake indicated. The disc has radius R and area A, while A_1 is the area of the far wake with radius R_1. In the remainder the index 0 is used for flow variables in the undisturbed, upstream flow. The fully developed far wake is indicated by the index 1, see figure 1. If there is no index, the variables are taken at the position of the actuator disc.

Wind Energ. Sci. Discuss., doi:10.5194/wes-2016-55, 2017
Manuscript under review for journal Wind Energ. Sci.
Published: 2 January 2017

eawe european academy of wind energy
Open Access WIND ENERGY SCIENCE DISCUSSIONS

2.2 The disc load

Only the pressure and the azimuthal velocity will be discontinuous across the disc with thickness ϵ for $\epsilon \to 0$, so integration of the axial and azimuthal component of (1) gives:

$$\frac{1}{\rho}\boldsymbol{F} = \frac{1}{\rho}\int_{\epsilon} \boldsymbol{f} dx = \boldsymbol{e}_x \frac{\Delta p}{\rho} + \boldsymbol{e}_\varphi v_x \Delta v_\varphi \tag{4}$$

$$= \boldsymbol{e}_x \Delta\left(\frac{H}{\rho} - \frac{1}{2}v_\varphi^2\right) + \boldsymbol{e}_\varphi v_x \Delta v_\varphi \tag{5}$$

where F denotes a surface load [N/m^2], Δ the difference between the down- and upwind side of the disc and $\boldsymbol{e}$ the unit vector. As $v_\varphi = 0$ at the upwind side of the disc $\Delta v_\varphi = v_\varphi$. In (5) the Bernoulli equation integrated across the disc thickness has been used:

$$\Delta p = \Delta H - \frac{1}{2}\rho v_\varphi^2. \tag{6}$$

The local power converted by the force field $\boldsymbol{f}$ is $\boldsymbol{f} \cdot \boldsymbol{v}$ which has to be equal to the local contribution to the torque, $r f_\varphi$, times rotational speed Ω. The converted power $\boldsymbol{f} \cdot \boldsymbol{v}$ becomes:

$$\boldsymbol{f} \cdot \boldsymbol{v} = \Omega r f_\varphi = (\boldsymbol{v} \cdot \boldsymbol{\nabla}) H. \tag{7}$$

This shows that the work done by the force field is expressed in a change in the total pressure or Bernoulli constant H. Integration of (7) across the thickness combined with the azimuthal component of (4) gives the general expression:

$$\Delta H = \frac{\Omega r}{v_x} F_\varphi = \rho \Omega r v_\varphi \tag{8}$$

and, with (3), for the Joukowsky disc:

$$\frac{1}{\rho}\Delta H = \frac{\Omega \Gamma}{2\pi}. \tag{9}$$

It follows that $\Delta H = constant$ by which (6) shows that any non-uniformity in the pressure jump is due to creation of swirl across the disc. The swirl-pressure jump does not change H so does not contribute to the conversion of power, so (6) may be interpreted as $\Delta p = \Delta p_{Hconversion} + \Delta p_{Hconserving}$. The sign conventions are that the rotational speed $\Omega > 0$ and $\Gamma < 0$ so $\Delta H < 0$ implying that energy is extracted from the flow.

2.3 The far wake

With the conservation of circulation:

$$r v_\varphi = r_1 v_{\varphi,1} \tag{10}$$

the Bernoulli equation (9) is written as:

$$\frac{1}{\rho}(p_0 - p_1) = \frac{1}{2}\left(v_{x,1}^2 - U_0^2 + v_{\varphi,1}^2\right) - \frac{\Omega \Gamma}{2\pi}. \tag{11}$$

Wind Energ. Sci. Discuss., doi:10.5194/wes-2016-55, 2017
Manuscript under review for journal Wind Energ. Sci.
Published: 2 January 2017

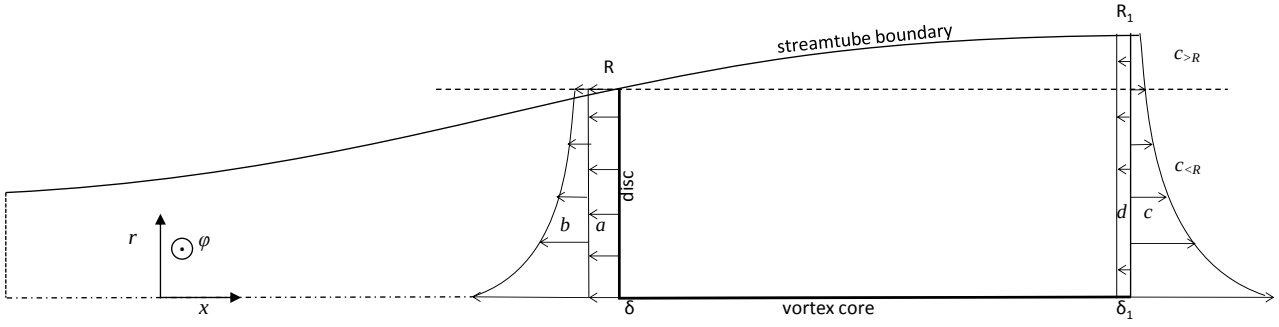

Figure 1. Pressure distributions acting in the momentum balance. The arrows give the direction of the pressure fields acting on the flow. The meaning of a, b, c and d is given in the main text.

Differentiating with respect to r and combining it with the radial pressure equilibrium in the far wake:

$$\frac{\partial p_1}{\partial r_1} = -\rho \frac{v_{\varphi,1}^2}{r_1} \tag{12}$$

it is clear that $v_{x,1}$ is constant. By this (11) can be written as:

$$p_1 - p_0 = -\frac{1}{2}\rho v_{\varphi,1}^2 + p^*. \tag{13}$$

At the wake boundary the pressure has to be undisturbed (p_0), so $p^* = \frac{1}{2}\rho v_{\varphi,R_1}^2$ and, with (3):

$$p_1 - p_0 = -\frac{1}{2}\rho v_{\varphi,1}^2 + \frac{1}{2}\rho \left(\frac{\Gamma}{2\pi R_1}\right)^2. \tag{14}$$

This shows that the pressure variation in the far wake is is caused only by the swirl. By merging (14) with (9) and (11) the second term at the right hand side appears as a loss in H due to swirl:

$$\Delta H = \frac{1}{2}\left(v_{x_1}^2 - U_0^2\right) - \frac{1}{2}\rho \left(\frac{\Gamma}{2\pi R_1}\right)^2. \tag{15}$$

3 Momentum theory

3.1 The momentum, mass and energy balance

The momentum equation drawn on the stream-tube as control volume, see figure 1, is written as:

$$T - \int_{A_1} (p_1 - p_0)\, dA_1 = \rho \int_{A_1} v_{x,1}\left(v_{x,1} - U_0\right) dA_1 \tag{16}$$

where T is the thrust [N] being the integrated pressure jump across the disc. It is convenient to split A and A_1 in two parts: the area inside the vortex core, so $r < \delta$ or δ_1, and outside of it $\delta < r < R$ or $\delta_1 < r_1 < R_1$. Irrespective of the choice for δ/δ_1,

Wind Energ. Sci. Discuss., doi:10.5194/wes-2016-55, 2017
Manuscript under review for journal Wind Energ. Sci.
Published: 2 January 2017

eawe european academy of wind energy
Open Access WIND ENERGY SCIENCE DISCUSSIONS

in the limit $\delta \to 0$ the core area only contributes to the momentum balance when the pressure or momentum flux is of order $O(\delta^2)$ or higher. In Sørensen and van Kuik (2011) this is analysed for the Rankine root vortex, showing that this is not the case. The same holds for the energy balance. Consequently in the remainder of the present analysis the flow region $r < \delta$ or δ_1 is discarded, with an exception for section 3.2.

Figure 1 shows the pressure distributions appearing in the left hand side of (16) including the thrust:

a) constant pressure jump across the disc giving the jump in Bernoulli parameter H according to the first term at the right hand side of (6).

b) pressure distribution due to jump in v_φ according to the second term at the right hand side of (6). This term conserves H.

c) the same pressure distribution in the far wake due to the v_φ distribution according to the first term at the right hand side of (14), conserving H.

d) constant pressure to achieve $p_1 - p_0 = 0$ according to the second term at the right hand side of (14) or (15).

When these contributions are expressed in Γ by (3) and (8), integrated, subjected to $\lim \delta \to 0$, substituted in (16) and divided by the disc surface πR^2 the result is:

$$\underset{a}{\frac{\Omega\Gamma}{2\pi}} - \underset{d}{\frac{1}{2}\left(\frac{\Gamma}{2\pi R}\right)^2} - \underset{b}{\left(\frac{\Gamma}{2\pi R}\right)^2 \int_\delta^R \frac{dr}{r}} + \underset{c}{\left(\frac{\Gamma}{2\pi R}\right)^2 \int_{\delta_1}^{R_1} \frac{dr_1}{r_1}} = v_{x,1}\left(v_{x,1} - U_0\right)\left(\frac{R_1}{R}\right)^2 \tag{17}$$

where the terms in the left hand side have been named in accordance with figure 1. The mass balance is:

$$\frac{\overline{v_x}}{v_{x,1}} = \left(\frac{R_1}{R}\right)^2 \tag{18}$$

with the bar above v_x indicating that it is the average value. The energy balance follows from (15):

$$\frac{\Omega\Gamma}{2\pi} - \frac{1}{2}\left(\frac{\Gamma}{2\pi R_1}\right)^2 = \frac{1}{2}\left(v_{x,1}^2 - U_0^2\right). \tag{19}$$

Mixing (17) and (18) simplifies the right hand side of the momentum balance yielding:

$$\frac{\Omega\Gamma}{2\pi} - \frac{1}{2}\left(\frac{\Gamma}{2\pi R}\right)^2 - \left(\frac{\Gamma}{2\pi R}\right)^2 \left[\int_\delta^R \frac{dr}{r} - \int_{\delta_1}^{R_1} \frac{dr_1}{r_1}\right] = \overline{v_x}\left(v_{x,1} - U_0\right). \tag{20}$$

The non-dimensional tip speed ration $\lambda = \frac{\Omega R}{U_o}$, and non-dimensional vortex $q = \frac{-\Gamma}{2\pi R U_o}$ are introduced. As $\Gamma < 0$ $q > 0$. Furthermore from here on $\overline{v_x}$ and $v_{x,1}$ indicate the dimensionless value $\frac{\overline{v_x}}{U_0}$ respectively $\frac{v_{x,1}}{U_0}$. Herewith (9) becomes:

$$\frac{1}{\rho}\frac{\Delta H}{U_0^2} = -\lambda q, \tag{21}$$

Wind Energ. Sci. Discuss., doi:10.5194/wes-2016-55, 2017
Manuscript under review for journal Wind Energ. Sci.
Published: 2 January 2017

eawe european academy of wind energy
Open Access WIND ENERGY SCIENCE DISCUSSIONS

and the momentum balance:

$$\lambda q + \frac{1}{2}q^2 + q^2\left[\ln\frac{R}{\delta} - \ln\frac{R_1}{\delta_1}\right] = \overline{v_x}\,(1 - v_{x,1}) \tag{22}$$

as well as the energy balance:

$$2\lambda q + q^2\left(\frac{R}{R_1}\right)^2 = \left(1 - v_{x,1}^2\right). \tag{23}$$

These equations can be solved for $\overline{v_x}$ once the term within the square brackets is known or more precisely: when the vortex core development is known. When $\overline{v_x}$ is known the power coefficient $C_p = P/(\frac{1}{2}\rho U_0^3 \pi R^2)$ follows by integration of (7) on the disc area:

$$C_p = 2\lambda q \overline{v_x}. \tag{24}$$

The thrust coefficient $C_T = T/(\frac{1}{2}\rho U_0^2 \pi R^2)$ contains the contributions a and b shown in figure 1, here denoted as ΔH respectively $\Delta\varphi$:

$$C_T = C_{T,\Delta H} + C_{T,\Delta\varphi} = 2\lambda q + q^2 \ln\left(\frac{R}{\delta}\right)^2. \tag{25}$$

3.2 The choice of the vortex core model

The momentum theory results are very sensitive to the choice of δ and δ_1 because of the logarithmic singularity in (22) for $\delta, \delta_1 \to 0$. This is in contrast to real instead of inviscid flows where viscosity removes the singularity. Furthermore, in the numerical potential flow model, presented in section 4, the vortex core size is not a parameter at all. The momentum balance (22) gives 2 possibilities to remove the impact of the singular behaviour from the momentum balance: either $\delta/R = \delta_1/R_1$ or $\delta = \delta_1$. In Sørensen and van Kuik (2011) the first possibility is assumed: the core diameter scales with the radius of the wake because of mass conservation. The two terms within the square brackets of (22) cancel each other completely so only pressure distributions a and d appear in the momentum balance. This holds for $\delta \to 0$ as well as for $\delta \neq 0$. However, this choice assumes that $\overline{v_{x,core}} = \overline{v_x}$, which is is not correct. The distribution $v_x(r)$ is known from calculations like in van Kuik and Lignarolo (2016) showing that for small r $v_x > \overline{v_x}$. As the velocity at both sides of the core boundary are equal, $v_{x,core} > \overline{v_x}$ which invalidates the assumption $\delta/R = \delta_1/R_1$.

The choice for $\delta = \delta_1$, so for a constant vortex core diameter, will be applied in the next section. Like for the model applied in Sørensen and van Kuik (2011) it is clear that this vortex core model can not satisfy the invsicid equations of motions: mass conservation makes a decelerating vortex core grow in diameter. However, the following analysis shows that the core with constant size represents best the effect of a smooth distribution of v_φ. Figure 2.8 in Alekseenko et al. (2007) shows the development over time of v_φ due to diffusion. Assuming that time may be replaced by downstream distance divided by velocity, figure 2 shows qualitatively the development of v_φ from disc to wake, both for inviscid and viscous flows. For $r < r^*$ the flow is assumed to have a viscous character while $v_{\varphi,1} = v_\varphi$ for $r^* < r < R$. To allow for other distributions of v_φ than (3) plus the

Wind Energ. Sci. Discuss., doi:10.5194/wes-2016-55, 2017
Manuscript under review for journal Wind Energ. Sci.
Published: 2 January 2017

eawe european academy of wind energy
Open Access WIND ENERGY SCIENCE DISCUSSIONS

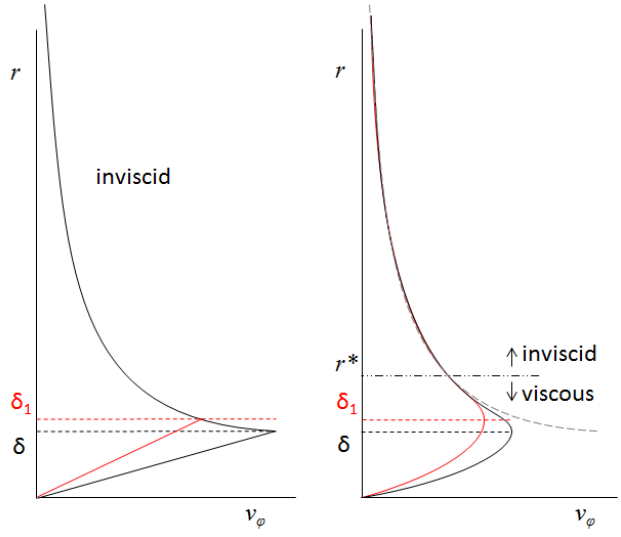

Figure 2. Qualitative sketch of the inviscid distribution of v_φ and the partly inviscid, partly viscous distribution.

Rankine vortex core, first the third term at the left hand side of (20) is reformulated in terms of v_φ:

$$-\frac{1}{R^2}\left[\int_0^R v_\varphi^2 r dr - \int_0^{R_1} v_{\varphi,1}^2 r dr\right] = \frac{1}{R^2}\left[\int_R^{R_1} v_{\varphi,1}^2 r dr - \int_0^{r^*}\left(v_\varphi^2 - v_{\varphi,1}^2\right) r dr\right] \tag{26}$$

with the lower bound of the integrals at the left hand side set to 0. The first integral at the right hand side is independent of a core model, but the second integral is. In Alekseenko et al. (2007) the development of a viscous vortex core is treated. For a specific accelerating vortex flow, the Burgers vortex, the diffusion and stretching counteract in such a way that the distribution of $v_\varphi(r)$ is invariant, see Alekseenko et al. (2007), so $v_\varphi = v_{\varphi 1}$ for $r < r^*$. For a decelerating vortex such a solution is not known. The vortex is compressed giving a similar vorticity spreading effect as diffusion. As it is not known what $v_{\varphi,\max}/v_{\varphi 1,\max}$ and δ/δ_1 are, the difference-integral in (26) cannot be evaluated without detailed calculations. However, as viscosity keeps the pressure and v_φ limited the second integral in the right hand side of (26) will not not contribute when $\delta, \delta_1 \ll R, R_1$. Then the first integral remains so, in dimensionless form:

$$-\frac{1}{R^2}\left[\int_0^R v_\varphi^2 r dr - \int_0^{R_1} v_{\varphi,1}^2 r dr\right] = q^2 \ln\frac{R}{R_1}. \tag{27}$$

The same result is obtained in the inviscid model of a potential vortex plus Rankine vortex core by assuming $\delta = \delta_1$, as is clear by (22). This shows that an inviscid core with an infinitely small but constant radius represents best the behaviour of a viscous vortex core, although verification by viscous actuator disc calculations is to be done. This model will be applied in the next section.

Wind Energ. Sci. Discuss., doi:10.5194/wes-2016-55, 2017
Manuscript under review for journal Wind Energ. Sci.
Published: 2 January 2017

eawe european academy of wind energy
Open Access WIND ENERGY SCIENCE DISCUSSIONS

3.3 Joukowsky actuator disc momentum theory with swirl

With $\delta = \delta_1 \to 0$ contribution b is cancelled by $c_{<R}$ which is the part of c up to $r_1 = R$. Now the pressure fields a, $c_{>R}$ and d appear in the momentum balance. The term with square bracket in (22) becomes:

$$-q^2 \ln\left(\frac{R_1}{R}\right) = -\frac{q^2}{2} \ln\left(\frac{R_1}{R}\right)^2 \tag{28}$$

and the momentum balance, making use of (18):

$$2\lambda q + q^2\left(1 - \ln\left(\frac{\overline{v_x}}{v_{x,1}}\right)\right) = 2\overline{v_x}\left(1 - v_{x,1}\right). \tag{29}$$

The energy balance (23) is unchanged.

By mixing (23) and (29) the velocity at the disc can be written as:

$$\overline{v_x} = \frac{1}{2}\left(v_{x,1}+1\right)\frac{\lambda q + \frac{1}{2}q^2\left(1 + \ln\left(\frac{R}{R_1}\right)^2\right)}{\lambda q + \frac{1}{2}q^2\left(\frac{R}{R_1}\right)^2}. \tag{30}$$

As $(1+\ln(R/R_1)^2) < (R_1/R)^2$ for $R < R_1$ the ratio is < 1. Consequently $\overline{v_x} < 0.5\left(v_{x,1}+1\right)$. The ratio in (30) is the ratio between the left hand side of the momentum balance (22) and energy balance (23) or, in other words, between the total load exerted on the flow in the stream-tube control volume and the non-conservative load which is the load performing work. By this, (30) is equivalent to equation 6 of van Kuik and Lignarolo (2016), where the distinction between the conservative and non-conservative loads is used to explain the results of the momentum theory applied to an annulus of the stream-tube.

An analytical solution of (23) and (29) is not found. An implicit expression of $v_{x,1}$ in the independent variables λ, q is obtained by writing (23) as an expression for $\overline{v_x}$ with the help of (18) and substitute this in (29):

$$\frac{\left(1-v_{x,1}\right)v_{x,1}q^2}{1+2\lambda q - v_{x,1}^2} = \left(q\lambda - \frac{1}{2}q^2\left(1 - \ln\left(\frac{q^2}{1+2\lambda q - v_{x,1}^2}\right)\right)\right). \tag{31}$$

This can be solved numerically for $v_{x,1}$. The wake expansion follows by (23) and the velocity at the disc by (29). Finally C_p is given by (24).

3.4 Limit values of the Joukowsky momentum theory for $\lambda \to 0$, $\lambda \to \infty$ and for maximum C_p

For large values of λ the wake angular momentum should go to 0, and the momentum theory should become the one-dimensional theory yielding the well-known Betz-Joukowsky maximum value for C_p. According to (21) q is inversely proportional to λ for constant ΔH or λq. In the balances (23) and (29) the q^2 terms vanish for $\lambda \to 0$ with which indeed the momentum theory without wake swirl is recovered.

For the limit $\lambda \to 0$ flow states with $\lambda q = constant$ are studied. The energy balance (23) shows that the highest value for $q^2(R/R_1)^2$ is obtained for $v_{x,1} = 0$:

$$2\lambda q + q^2\left(\frac{R}{R_1}\right)^2 = 1. \tag{32}$$

Wind Energ. Sci. Discuss., doi:10.5194/wes-2016-55, 2017
Manuscript under review for journal Wind Energ. Sci.
Published: 2 January 2017

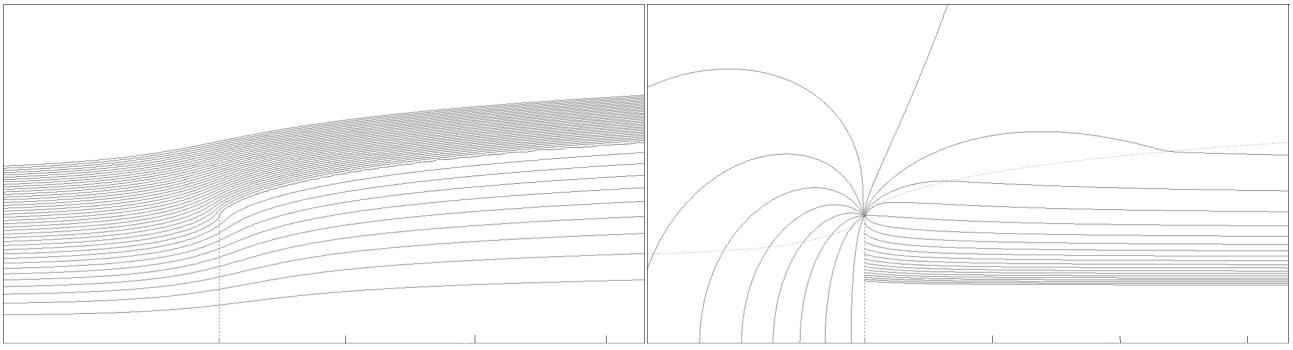

Figure 3. Streamlines with $\Delta\psi = 0.1\Delta\psi_{wake}$ and isobars with $\Delta p = 0.1\Delta H$ for $\Delta H/(\frac{1}{2}\rho U_0^2) = -0.8888$ and $\lambda = 0.731$. Isobars close to the wake axis are not plotted. Ticks at the axes are at a $1R$ interval.

The right hand side of the momentum balance is 0 for $v_{x,1} = 0$, see (17), by which it becomes):

$$2\lambda q + q^2\left(1 - \ln\left(\frac{R_1}{R}\right)^2\right) = 0. \tag{33}$$

Elimination of q^2 from (32) and (33) gives the wake expansion for the highest q - lowest λ:

$$\left(\frac{R_1}{R}\right)^2\left(1 - \ln\left(\frac{R_1}{R}\right)^2\right) = \frac{2\lambda q}{2\lambda q - 1}. \tag{34}$$

As an example, $2\lambda q = 8/9$ results in $\frac{R_1}{R} = 2.77$, $q = 0.924$ by (32) and $\lambda = 0.48$. Although the wake expansion is significant, both $\overline{v_x}$ and $v_{x,1}$ are 0, but the ratio of $\frac{\overline{v_x}}{v_{x,1}} \to 7.69$. This flow state is characterized by a full blockage by the disc, creating a wake with azimuthal flow only, so there is no change in axial momentum. The associated pressure distributions in the wake and at the disc balance each other. A lower value of λ is not possible for this value of λq. For $\lambda q = 0$ with $\lambda = 0$, (34) gives $\ln\left(\frac{R_1}{R}\right)^2 = 1$, (32) gives $\frac{R_1}{R} = q = \sqrt{e} = 1.648$ although $v_x = v_{x,1} = 0$. In the wake only the azimuthal velocity is non-zero, reaching $\frac{q}{2\pi R_1} = 1$ at the far wake boundary $r = R_1$. The wake expansion is close the experimental value ≈ 1.6 of the wake expansion behind a solid disc reported in Craze (1977).

$C_{p,max}(\lambda)$ is obtained by optimizing the solutions for fixed λ varying q.

4 Potential flow calculations

The computer code described in van Kuik and Lignarolo (2016) has been adapted to include wakes with swirl. Axial and radial velocities are calculated by summation of the induction by each of the several thousand vortex rings which constitute the wake boundary. The azimuthal velocities are calculated by (3). The shape and strength of the vortex rings are adapted in the convergence scheme to satisfy the two boundary conditions: zero pressure jump across the wake boundary, and zero cross flow. The first boundary condition $\Delta p_{wake-boundary} = 0$ is expressed in $|\boldsymbol{v}|$ and input parameter ΔH: $\Delta(\frac{1}{2}\rho|\boldsymbol{v}|^2) - \Delta H = 0$. In van Kuik and Lignarolo (2016) $\boldsymbol{v}$ only had an axial and radial component, now the azimuthal component enters the boundary

Wind Energ. Sci. Discuss., doi:10.5194/wes-2016-55, 2017
Manuscript under review for journal Wind Energ. Sci.
Published: 2 January 2017

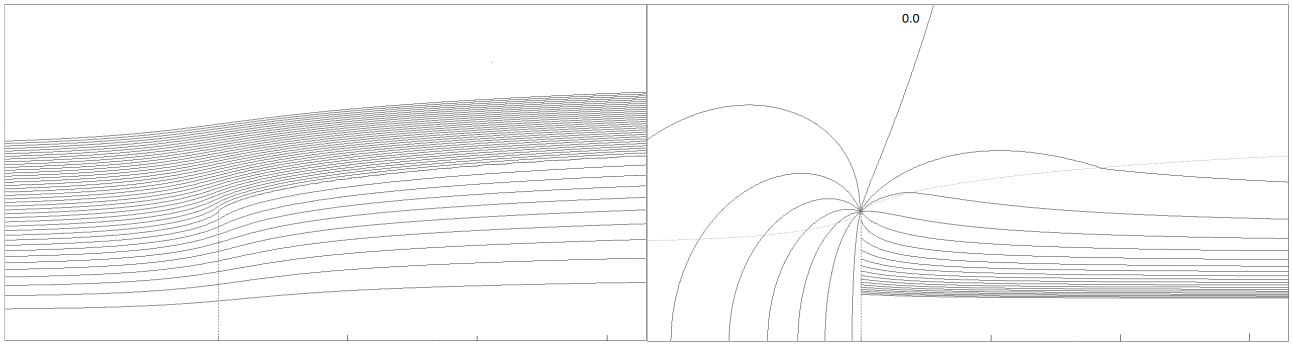

Figure 4. Streamlines with $\Delta\psi = 0.1\Delta\psi_{wake}$ and isobars with $\Delta p = 0.1\Delta H$ for $\Delta H/(\frac{1}{2}\rho U_0^2) = -0.8888$ and $\lambda = 1.018$. Isobars close to the wake axis are not plotted. Ticks at the axes are at a $1R$ interval.

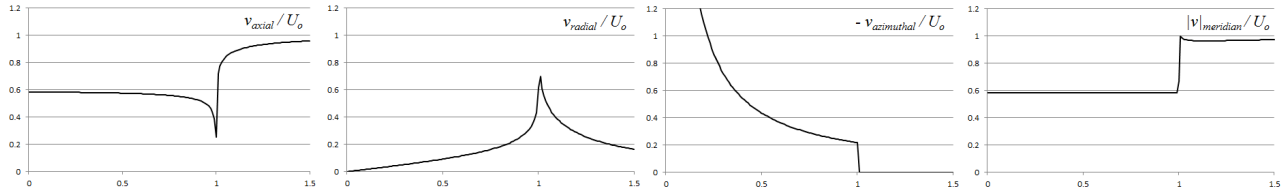

Figure 5. The velocity components at $x = 0$ for $\Delta H/(\frac{1}{2}\rho U_0^2) = -0.8888$ and $\lambda = 1.018$. $|v|_{meridian}$ is $\sqrt{{v_x}^2 + {v_r}^2}$. The horizontal axis displays r/R.

condition. The strength of the vortex at the axis follows from (21) expressed in H and the second input parameter λ: $q = -\Delta H/(\rho U_0^2 \lambda)$. Apart from these changes the code and the numerical parameters are unmodified. The results satisfy the same accuracy requirements as described in van Kuik and Lignarolo (2016). Figure 3 and figure 4 show the streamlines, expressed in the stream-function Ψ, and isobars of the disc flow with $\Delta H/(\frac{1}{2}\rho U_0^2) = -0.8888$ and $\lambda = 0.731$ respectively 1.018. The isobars in the wake show the pressure gradient due to the swirl.

5 Constant meridian velocity at the disc

As shown in figures 3 and 4 the pressure at the upstream side of the disc is constant, which implies, by the Bernoulli equation, that the absolute velocity $|\boldsymbol{v}|$ upstream of the disc is constant. Figure 5 shows the values of the axial, radial and azimuthal velocity component at the disc as well as the absolute value $|v|_{meridian} = \sqrt{{v_x}^2 + {v_r}^2}$. The fact that $|v|_{meridian}$ is constant confirms the findings in van Kuik and Lignarolo (2016) where the same result was found for actuator disc flows without swirl, so is independent of λ. The explanation given in van Kuik and Lignarolo (2016) is now extended to include discs with swirl.

The radial component of (1) just upstream of the disc is:

$$\rho v_s \frac{\partial v_r}{\partial s} = -\frac{\partial p}{\partial r} \tag{35}$$

Wind Energ. Sci. Discuss., doi:10.5194/wes-2016-55, 2017
Manuscript under review for journal Wind Energ. Sci.
Published: 2 January 2017

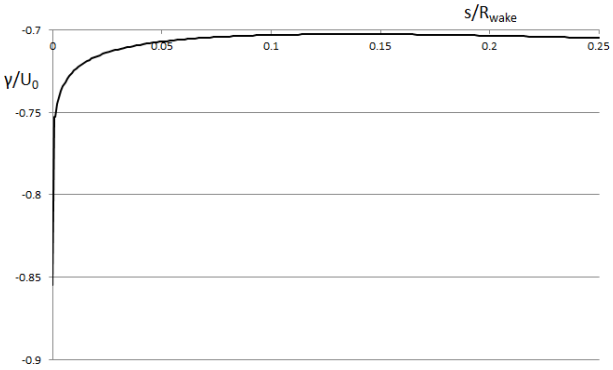

Figure 6. Strength of the vortex sheet as a function of the distance s from the leading edge measured along the sheet, for $\Delta H/(\frac{1}{2}\rho U_0^2) = -0.8888$ and $\lambda = 1.018$..

with s being the coordinate along the streamline and r the radial coordinate. The pressure does not depend on r when it is shown that the radial velocity reaches a maximum at the disc when following a streamline. Along any streamline passing the disc, v_r increases when the position of observation s_0 travels from far upstream to the disc s_{disc}, due to the decreasing distance to the vorticity γ in the wake boundary, so $\partial v_r/\partial s > 0$. At the streamline in the wake two regions can be distinguished: the vorticity between s_{disc} and s_0 induces a negative v_r so contributes to $\partial v_r/\partial s < 0$, while the induction by the vorticity downstream of s_0 will vary only slightly as γ is non-uniform. The result is that $\partial v_r/\partial s = 0$ at the disc position, so by (35) the pressure upstream of the disc is constant and by the Bernoulli equation $|v|_{meridian}$ is constant, QED.

Figure 6 shows the calculated strength of the vortex sheet for the load case of figures **??** and 5, confirming the reasoning. With $|\gamma|$ having a maximum at its leading edge, the non-uniformity of γ contributes to a negative induction of v_r at streamline positions $s_0 > s_{disc}$. It should be noted that the distribution in figure 6 does not show the irregular behaviour at the leading edge as shown in figure 9 of van Kuik and Lignarolo (2016). The explanation is that the distance between the first vortex rings in this previous paper is smaller than the radius of the vortex ring core, leading to this irregularity. Calculations with a smaller core size, not yet reported, have removed this irregularity, thereby not having impact on the flow pattern and numerical results. In the present calculation the distance between rings is always larger than the radius of the core of the vortex ring.

Now the pressure at the upstream side of the disc is known to be constant, the radial derivative of (6) becomes:

$$\frac{\partial p_-}{\partial r} = -\rho\frac{v_\varphi^2}{r} \tag{36}$$

with p_- being the pressure at the downstream side of the disc. This is the radial equilibrium expression (12) for the flow in the wake. Apparently the the radial distribution of p is linked to v_φ only, not to the other velocity components.

Wind Energ. Sci. Discuss., doi:10.5194/wes-2016-55, 2017
Manuscript under review for journal Wind Energ. Sci.
Published: 2 January 2017

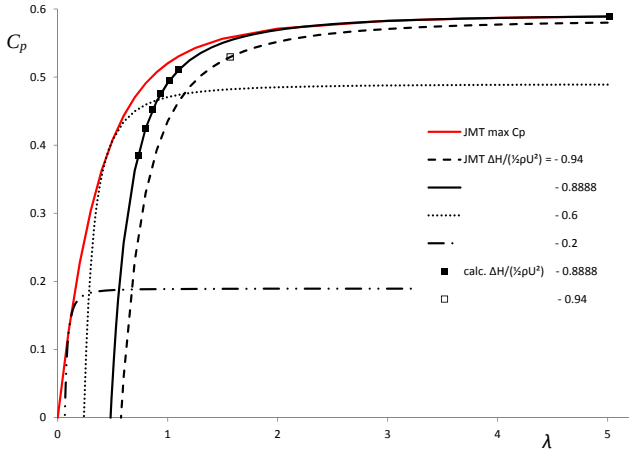

Figure 7. The Joukowsky momentum theory results compared with potential flow calculations.

6 Results

Figure 7 shows the comparison of the Joukowsky Momentum Theory and the potential flow results. The correspondence between both is excellent. A comparison with the $C_{p,max} - \lambda$ curve for discs having a modified Betz-Goldstein distribution of the circulation is shown in figure 8. As shown by Okulov and Sørensen (2008); Okulov (2014) the original Betz-Goldstein solution for a rotor with a finite number of blades resulted in $C_{p,max} = 1$, as the pitch of the helicoidal wake was based on the undisturbed velocity. With the pitch based on the velocity in the rotor plane, Okulov (2014) showed that $C_{p,max}$ reaches the well known Betz-Joukowsky maximum $16/27$ for high λ. The $C_{p,max} - \lambda$ curve of this corrected solution expanded to a rotor with an infinite number of blades is shown in figure 3 of Okulov (2014). An alternative solution is published in Wood (2015) where the Goldstein formulation is adapted to allow for non-zero torque when $\lambda \to 0$. A comparison of the Joukowsky maximum C_p curve and corresponding Betz-Goldstein-Okulov/Wood curves is given in figure 8. The Joukowsky distribution gives higher $C_{p,max}$ than the Betz-Goldstein based distributions, with the difference vanishing for higher λ. This is confirmed by Okulov and Sørensen (2010) where rotors with a finite number of blades having a Joukowsky and Betz-Goldstein based distribution have been compared.

7 Conclusions

- An actuator disc momentum theory including wake swirl has been developed resulting in the physically plausible result that $C_p \to 0$ in the limit $\lambda \to 0$. For high λ the theory reproduces the results of the classical momentum theory without swirl.

- The novelty in the method is the removal from the momentum balance of the singular behaviour of the pressure near the wake centreline vortex, giving rise to non-physical results in several previously published methods. This removal is

Wind Energ. Sci. Discuss., doi:10.5194/wes-2016-55, 2017
Manuscript under review for journal Wind Energ. Sci.
Published: 2 January 2017

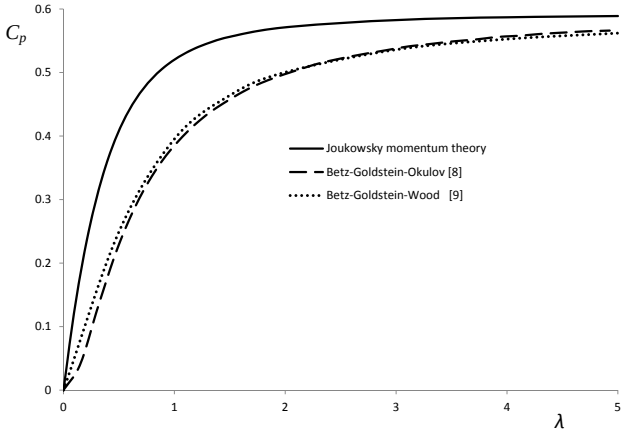

Figure 8. The Joukowsky actuator disc results compared with the Betz-Goldstein solutions of Okulov (2014) and Wood (2015) for rotors with an infinite number of blades.

done by applying a vortex core with constant diameter δ. Support for this is found in the absence of singular flow when viscous core development is considered.

- The momentum theory results are very accurately confirmed by potential flow field calculations.
- At the actuator disc the velocity in the meridian plane is constant.
- The Joukowsky momentum theory results are higher than the equivalent results for rotors with an infinite number of blades optimized for modified Betz-Goldstein solutions.

Acknowledgements. Thanks go to Jens Norkær Sørensen, DTU, for the discussions about the modified momentum theory and to Valery Okulov, DTU, and David Wood, University of Calgary, for a discussion on the Betz-Goldstein solution and for providing the data shown in figure 8.

Wind Energ. Sci. Discuss., doi:10.5194/wes-2016-55, 2017
Manuscript under review for journal Wind Energ. Sci.
Published: 2 January 2017

eawe european academy of wind energy
Open Access WIND ENERGY SCIENCE DISCUSSIONS

References

Alekseenko, S. V., Kuibin, P. A., and Okulov, V. L.: Theory of Concentrated Vortices, Springer Verlag, Berlin, Heidelberg, 2007.

Betz, A.: Schraubenpropeller mit geringstem Energieverlust, Vier Abhandlungen zur Hydrodynamik und Aerodynamik, Reprint of 4 famous papers by Universitätsverlag Göttingen, 1927.

Craze, D.: On the near wake behind a circular disc, 6th Australasian Hydraulics and Fluid Mechanics Conference, pp. 282–286, 1977.

de Vries, O.: Fluid dynamic aspects of wind energy conversion, AGARDograph 243, AGARD, Amsterdam, 1979.

Goldstein, S.: On the vortex theory of screw propellers, Proc. R. Soc. Lond. A, 123, 440–465, 1929.

Joukowsky, J. N.: Vortex theory of the screw propeller IV, Trudy Avia Raschetno- Ispytatelnogo Byuro 1918;3:1–97 (in Russian) Also published in Gauthier-Villars et Cie. (eds). Théorie Tourbillonnaire de l'Hélice Propulsive, Quatrième Mémoire. 123–146:, 1918.

Okulov, V. L.: Limit cases for rotor theories with Betz optimization, Journal of Physics: Conference Series, 524, 012 129, doi:10.1088/1742-6596/524/1/012129, 2014.

Okulov, V. L. and Sørensen, J. N.: Refined Betz limit for rotors with a finite number of blades, Wind Energy, 11, 415–426, doi:10.1002/we.274, 2008.

Okulov, V. L. and Sørensen, J. N.: Maximum efficiency of wind turbine rotors using Joukowsky and Betz approaches, Journal of Fluid Mechanics, 649, 497–508, doi:10.1017/S0022112010000509, 2010.

Okulov, V. L., Sørensen, J. N., and Wood, D.: The rotor theories by Professor Joukowsky: Vortex Theories, Progress in Aerospace Sciences, 73, 19–46, doi:10.1016/j.paerosci.2014.10.002, 2015.

Sharpe, D. J.: A general momentum theory applied to an energy-extracting actuator disc, Wind Energy, 7, 177–188, doi:10.1002/we.118, 2004.

Sørensen, J. N.: General Momentum Theory for Horizontal Axis Wind Turbines, Springer International Publishing, Heidelberg, doi:10.1007/978-3-319-22114-4, 2015.

Sørensen, J. N. and van Kuik, G. A. M.: General momentum theory for wind turbines at low tip speed ratios, Wind Energy, 14, 821–839, doi:10.1002/we.423, 2011.

van Kuik, G. A. M. and Lignarolo, L. E. M.: Potential flow solutions for energy extracting actuator disc flows, Wind Energy, 19, 1391–1406, doi:10.1002/we.1902, 2016.

van Kuik, G. A. M., Sørensen, J. N., and Okulov, V. L.: Rotor theories by Professor Joukowsky: Momentum theories, Progress in Aerospace Sciences, 73, 1–18, doi:10.1016/j.paerosci.2014.10.001, 2015.

Wood, D. H.: Including swirl in the actuator disk analysis of wind turbines, Wind Engineering, 31, 317–323, 2007.

Wood, D. H.: Maximum wind turbine performance at low tip speed ratio, Journal of Renewable and Sustainable Energy, 7, 053 126, doi:10.1063/1.4934895, 2015.

Xiros, M. I. and Xiros, N. I.: Remarks on wind turbine power absorption increase by including the axial force due to the radial pressure gradient in the general momentum theory, Wind Energy, 10, 99–102, doi:10.1002/we.203, 2007.